Physics – Uspekhi **47** (2) 187 – 194 (2004)

PHYSICS OF OUR DAYS

PACS numbers: 95.85.Bh, 98.70.Vc, **98.80. – k**

Anisotropy and polarization of cosmic microwave background: state of the art

M V Sazhin

DOI: 10.1070/PU2004v047n02ABEH001630

Contents

Abstract. The anisotropy and polarization of cosmic microwave background radiation provide the most powerful tools for modern cosmology. At present, many experiments for observing these phenomena are either being conducted or prepared, which holds promise for yielding the fundamental parameters of the present and early universe; for shedding light on the crucial current problem of the existence of gravitational waves; and for solidly contributing to elementary particle and high energy physics. In the present paper the formation mechanisms of anisotropy and polarization are briefly discussed. The latest experiments in the field, in particular the WMAP experiment aboard a special spacecraft, are given particular attention.

1. Introduction

We are living in an expanding Universe. Its kinematic and dynamic properties are characterized by the scale factor $a(t)$ and its dependence upon time. The ratio of the present-day scale factor to its value at some previous epoch is called the redshift of this epoque and is denoted by z.

In the past, when the scale factor was about 1000 times smaller than now, the Universe was filled by high-temperature plasma consisting of electrons, protons, massive weakly interacting particles, and photons. The number of photons was much larger than the number of baryons (by several billion times). This is why the Universe is called 'hot'. As the Universe expands, its temperature decreases and it cools down. While the expansion rate is much smaller than the characteristic rate of the establishment of thermodynamic equilibrium in the hot plasma, the plasma particles are in thermodynamic equilibrium. The photon is one such particle. It is these photons that are called 'relic' and are observed as the cosmic microwave background (CMB).

Despite the fact that the photon propagates in a vacuum with the speed of light, in a hot dense plasma photons move much slower due to scattering on electrons. When the Universe expands such that the plasma cools down to the recombination temperature, electrons start recombining with protons to form neutral hydrogen, and photons start propagating freely. Points from which photons reach the observer form the so-called 'surface of the last scattering'. This is the unique source in the Universe which encircles us from everywhere.

At the time of recombination, the temperature of the last scattering surface was about 3000 K. Now it is 1000 times smaller. This decrease occurred due to the expansion of the Universe.

The CMB has a unique property. Its temperature exhibits astonishing isotropy. It is isotropic with an accuracy of one part in 1000. Nevertheless, a small anisotropy still persists. The anisotropy is the temperature difference observed from different directions in the sky. Its value is approximately 3 mK. This is due to the Earth, the solar system, and our Galaxy moving through CMB with some peculiar velocity. Three mK is the kinetic component of the CMB anisotropy called the dipole anisotropy: ahead of us (in the direction of motion) the temperature is slightly higher, while behind us (in the opposite direction of motion) it is slightly smaller.

In addition to the kinetic component, the CMB anisotropy has potential terms which are due to gravitation fields of very large scales comparable to particle horizon or in other words, to the distance to the last scattering surface. The lowest harmonic in such a gravity field is a quadrupole. This is because [1] a gravity field possesses no dipole harmonic. The dipole harmonic emerges only in the fields that have charges with different charge to mass ratio. The gravity field is

M V Sazhin P K Sternberg Astronomical Institute,
M V Lomonosov Moscow State University,
119992 Moscow, Universitetskiĭ prosp. 13, Russian Federation
Tel. (7-095) 939 50 06
E-mail: sazhin@sai.msu.ru

Received 20 March 2003, revised 25 August 2003
Uspekhi Fizicheskikh Nauk **174** (2) 197 – 205 (2004)
Translated by K A Postnov; edited by M I Zel'nikov

[1] Here we remind the reader that all bodies have the same acceleration in a gravity field.

produced by masses which all have the same charge to mass ratio. The degree of inhomogeneity of the gravity field is characterized by tidal forces, the lowest harmonic of which is a quadrupole.

Let us consider the basic equation that describes the CMB anisotropy and principal physical effects that cause the anisotropy. The equation describing temperature changes in the direction of vector **e** reads

$$\frac{\delta T(\mathbf{e})}{T} = -\frac{1}{2}\int_{\eta_r}^{\eta_0} \mathrm{d}\eta\, \frac{\partial h_{ij}(\eta, \mathbf{r}(\eta))}{\partial \eta}\, e^i e^j + \frac{1}{4}\,\frac{\delta\rho_r}{\rho_r}\bigg|_r + \left(\mathbf{e}\,\frac{\mathbf{v}_r}{c}\right)\bigg|_r . \tag{1}$$

The first term in this equation describes the Sachs – Wolf effect [2], which was predicted at the beginning of the 1960s by Sachs and Wolf and is simply the fact that photons moving in changing gravitational potential either acquire or lose energy.

The second term is due to the Silk effect. Imagine that there are some density fluctuations at the last scattering surface. Fluctuations in the baryon density are accompanied by photon density fluctuations as (and this is firmly proved) the entropy across the space is also astonishingly homogeneous, to a much larger degree than CMB. The essence of the Silk effect is as follows. In a region with enhanced baryon contrast the contrast of photons is enhanced too.

The third term is due to the Doppler effect. The last scattering surface, more precisely, the matter which forms it, can move. If some part of this surface moves towards us then the photons it emits get bluer, if it moves away from us, the photons get redder. Depending upon the velocity, more precisely, upon the projection of the velocity vector on the line of sight, we observe a bluer or redder shift in the photon energy, and for temperature this appears as anisotropy in a given direction.

As the last scattering surface is a sphere, the simplest way to analyze the anisotropy of CMB is the expansion of the observed temperature fluctuations into spherical functions, which constitute the full and orthogonal set of functions on the sphere:

$$\delta T(\theta, \phi) = \sum_{l=2}^{\infty} a_{lm}\, Y_{lm}(\theta, \phi)\,, \tag{2}$$

where a_{lm} are coefficients called multipole coefficients and Y_{lm} are spherical harmonics. It should also be noted that it is more convenient to represent and compare results of observations and theoretical calculations in terms of quantities which are rotationally invariant and do not depend upon a particular choice of the reference frame. It is worth remembering that several frames are used in astronomy: the equatorial coordinate system connected with Earth, the ecliptic system related to the location of Earth's orbit, and the galactic system. In each of these systems coefficient a_{lm} will take different values. The point is that they are not rotationally invariant. So one usually chooses the so-called rotationally invariant quantity

$$C_l = \frac{1}{2l+1}\sum_{l=-m}^{l=m} |a_{lm}|^2 \tag{3}$$

which is adequate for the analysis. The spectrum is constructed for $l(l+1)C_l/2\pi$. This is due to the fact that when multiplying C_l by $l(l+1)$, the spectrum exhibits the so-called Harrison – Zel'dovich plateau which looks like a horizontal line. As we shall see, most experimental data on multipole CMB spectra use this normalization.

For more information on the modern concepts of the structure and evolution of the Universe see books [1 – 5].

2. Discovery of anisotropy and recent experiments

It should be mentioned that CMB, detected in 1965, has been the most significant discovery in cosmology since Hubble's discovery of the expanding Universe. The CMB dipole anisotropy (motion through CMB) was detected in 1972. (The present-day value of the dipole harmonic amplitude is ~ 3 mK.) After that, radio astronomers improved radiometers for 20 years and ultimately registered the CMB anisotropy at higher harmonics, which is related to primordial fluctuations of gravity field that provided us by information on the early Universe.

The large-scale CMB anisotropy was discovered in 1992 when analyzing data obtained by the 'Relikt' satellite. In January 1992, at a seminar at Sternberg Astronomical Institute, our group claimed to have detected the CMB anisotropy, although with a marginal signal-to-noise ratio on the order of three. We published a paper in *Soviet Astronomy Letters* and sent it in parallel to *Monthly Notices of Royal Astronomical Society* where it also appeared after several months [6, 7].

By that time, the NASA satellite COBE (from COsmic Background Explorer) was in orbit. It was an apparatus similar to the 'Relikt' satellite but with higher sensitivity. COBE had three frequency channels with two radiometers in each. Shortly after our paper [6], the COBE group published their results [8] and announced the detection of CMB anisotropy.

Multifrequency analysis allowed the COBE group to confidently separate the anisotropy at the last scattering surface from that of galactic and extra galactic radio emissions. This fact, as well as the higher signal-to-noise ratio achieved after the termination of the experiment (COBE operated more than 4 years), allowed the NASA scientists to relate the CMB anisotropy discovery with the COBE results.

Since 1992, many experiments have been performed to observe CMB anisotropy both from the ground and from balloons, but the sensitivity of radiometers in those experiments is approximately the same as in the 'Relikt' and COBE satellites. Nonetheless, the multipole spectrum was constructed, which coincided with the theoretical one displaying the Harrison – Zel'dovich plateau and containing the first Doppler peak (Fig. 1). However, data from these experiments have large uncertainties due to the low sensitivity of the radiometers used.

A new generation of radiometers was realized in the BOOMERang experiment [9]. In 1998, a balloon flight was undertaken, loaded with the BOOMERang experiment equipment. The balloon made a full circle above Antarctica which allowed the researchers to construct a radio brightness map of a small area in the sky. Only 5% of the full sky area was measured. Nevertheless, the area was successfully chosen such that there were no strong extragalactic radio sources and the synchrotron radiation intensity was minimal.

[2] In cosmology the redshift which causes the anisotropy is often called the Sachs – Wolf effect.

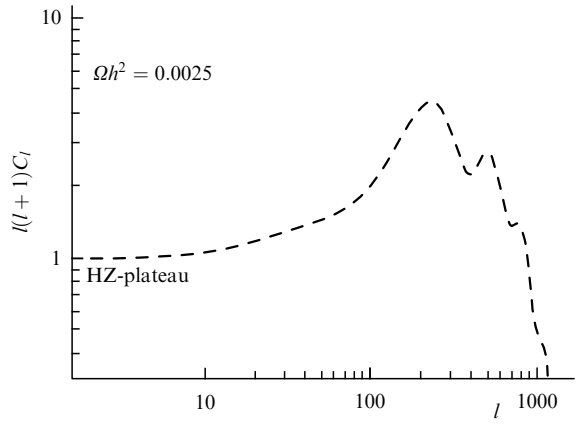

Figure 1. Theoretical spectrum of the CMB anisotropy according to the standard cosmological model.

As a result, the CMB anisotropy spectrum was measured (the so-called C_l-spectroscopy), which revealed the presence of the first, second, and third Doppler peaks. Presently, the experimentalists claim to observe five peaks. Since the size of the measured sky map was small, the minimal value of the multipole number measured in this experiment is $l \approx 26$. So the matching with the Harrison–Zel'dovich plateau was approximate.

Soon after that the Archeops balloon experiment was performed [10, 11] (see also the web-site of the Archeops experiment [12]). It was designed in France with the participation of many European researchers. Russian cosmologists A A Starobinsky and I A Strukov also took part in this experiment. This experiment is considered as the predecessor of the high-frequency part of the future 'Planck' experiment.

In the course of this experiment, several balloon flights were made, the last in February 2002. The balloon was launched in Sweden and landed in Norilsk.

Experimentalists rapidly processed the obtained data. A record sensitivity of about 100 μK was achieved. The outcome of this experiment was a sky map covering 30% of the total sky area with an angular resolution of 8 arc minutes at 143 GHz.

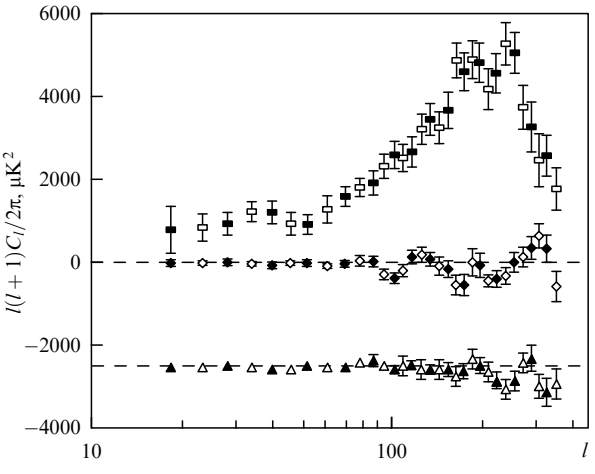

Figure 2. Multipole spectrum obtained by the 'Archeops' experiment.

The Archeops results are presented in Fig. 2. The value $l(l+1)C_l$ divided by 2π is plotted against l. The measurements allowed the determination of multipole amplitudes from $l = 10$ to $l \approx 150$. The fraction of the Harrison–Zel'dovich plateau, an almost constant value of $l(l+1)C_l$ from $l = 2$ to $l \approx 30$, is clearly seen in the figure. The residuals from two spectra obtained using two different methods (the bottom plot) is comparable to zero.

Using the C_l spectrum, one can determine the spectrum of fluctuations in the Universe, as well as global cosmological parameters: the total density of the Universe and its constituents, such as the baryon density, the density of dark matter, the density corresponding to the Λ-term, etc. For example, the location of the first Doppler peak allows the accurate determination of the total density of the Universe, while its amplitude provides the baryonic content.

Before passing to the WMAP experiment, it is necessary to describe one more experiment, called DASI [13, 14]. The point is that in this experiment CMB polarization was first detected. The CMB anisotropy itself is very tiny, the first Doppler peak amplitude is on the order of 75 μK, and the Harrison–Zel'dovich plateau amplitude is about 20 μK. In other words, the relative anisotropy is $\sim 10^{-5}$. The CMB polarization, which provides invaluable information on the modern and early Universe, has an even smaller amplitude.

In the DASI experiment, in which the CMB polarization was measured for the first time, the C_l-spectroscopy from $l = 150$ to $l = 1000$ was performed at different frequencies.

It should be remembered that electromagnetic radiation is characterized not only by intensity, but also by three Stokes parameters Q, U, and V. V is responsible for circular polarization, Q and U describe linear polarization. We remark from the very beginning that in CMB radiation only linear polarization forms during the recombination, when the optical depth for Thompson scattering changes from about 3 to 0.1, so cosmologists assume $V = 0$. The quantities Q, U, and V are second-rank tensors upon a sphere. The CMB intensity can be expanded in scalar spherical harmonics, while the values Q and U should be expanded in the so-called second-rank spin harmonics, which corresponds to rotationally invariant expansions of a second-rank tensor [15–17]:

$$Q \pm \mathrm{i}U = \sum_{l,m} a_{lm}^{\pm 2}\, Y_{lm}^{\pm 2}(\theta, \varphi)\,. \tag{4}$$

In addition to new functions, in which expansion is performed, the so-called E- and B-modes are distinguished in polarization [17]:

$$a_{lm}^{E} = \frac{1}{2}(a_{lm}^{+2} + a_{lm}^{-2})\,,$$
$$a_{lm}^{B} = \frac{\mathrm{i}}{2}(a_{lm}^{+2} - a_{lm}^{-2})\,. \tag{5}$$

These modes correspond to two quantities with principally different symmetry. The B-mode is anti-symmetric with respect to parity transformations. This is very important since the difference between the E and B modes will allow us in the future to distinguish the contribution of density perturbations to the anisotropy from that of gravitational waves. The point is that density perturbations generate *only* the E-mode of the CMB polarization, whereas gravitational waves generate both the E- and B-modes. So measuring the polarization allows the determination of the density perturbation spectrum separately from the gravitational wave spectrum.

DASI is the ground-based experiment performed at the South Pole. The experiment registered the *E*-mode of polarization. The *B*-mode was not detected. In order to make sure that what is observed is the polarization of radiation from the last scattering surface and not of the synchrotron radiation, researchers plot the so-called frequency index of the brightness temperature of the *E*-mode and check whether it is zero or not. For CMB the frequency index is exactly zero as the CMB temperature is the blackbody temperature and is independent of frequency, while the brightness temperature of any other radiation, for example, of synchrotron radiation, is a function of frequency.

3. The WMAP experiment

3.1 Description of the experiment

The name WMAP is abbreviated from Wilkinson Microwave Anisotropy Probe [18]. Initially, the satellite was named MAP. The famous scientist David Wilkinson, who was one of the authors of the MAP project, died in September 2002, and in his memory his pupils and collaborators decided to give his name to the MAP satellite.

The satellite represents an apparatus 830 kg in weight (Fig. 3). It was launched in 2001 to the point L2, which lies 1.5 million km away from Earth in the direction opposite the Sun.

The lifetime of the satellite at the working point was assumed to be at least 2 years, with three months added to bring it to the calculated point.

The satellite is devoted to measuring the CMB anisotropy and polarization. The main goal of the experiment is to construct an all-sky map with a sensitivity of not less than 20 μK per pixel [3] and systematical errors below 5 μK in each pixel. The receiver system of the satellite consists of two Gregory telescopes 1.4×1.6 m. Several radiometers tuned at different frequencies are installed in the telescope focus. The radiometers' characteristics are collected in Table 1.

Each frequency has its own name. The two lowest frequencies K and Ka serve for monitoring galactic emission, and the three highest frequencies Q, V, and W, are used to construct maps of emission from the last scattering surface (Fig. 4).

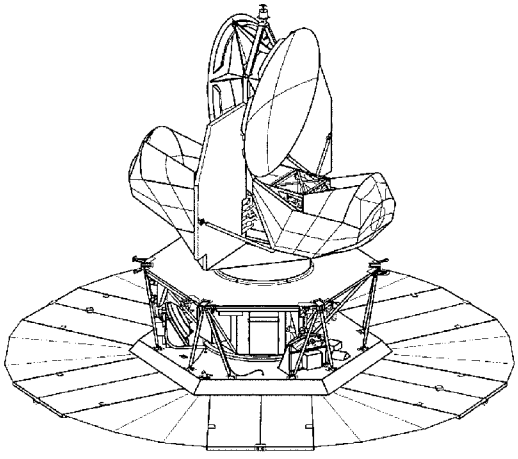

Figure 3. The WMAP satellite.

[3] Pixel is the element of the image corresponding to the resolution of the matrix receiving radiation.

Table 1

Frequency band	K	Ka	Q	V	W
Frequency, GHz	22	30	40	60	90
Wavelength, mm	13.6	10.0	7.5	5.0	3.3
Number of channels	4	4	8	8	16
Resolution, deg	0.93	0.68	0.53	0.35	0.23
Sensitivity, μK (pixel size $0.3 \times 0.3^\circ$)	~ 35	~ 35	~ 35	~ 35	~ 35

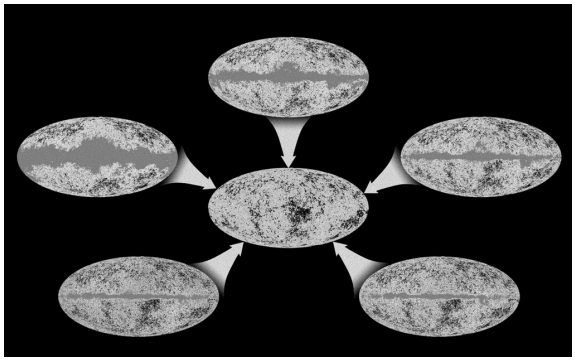

Figure 4. Sky maps obtained at different frequencies by WMAP (on the periphery). The synthetic sky map constructed from the maps at different frequencies is at the center.

In February 2003, the WMAP group published several papers with the first experimental results. In addition, a lot of information can be found on the web-page of the WMAP group [18], from which we borrowed the image of the WMAP satellite, δT maps, and plots of the anisotropy spectra and cross-correlation of the anisotropy and polarization.

3.2 Results of the first year of operation

Let us discuss the most important results from the cosmological point of view. The determination of the multipole spectrum is considered in paper [19]. To construct a map at any frequency, eight differential aggregates of radiometers were used. Each unit comprised two radiometers sensitive to mutually perpendicular modes of linear polarization.

After correcting all high-frequency maps for distributed galactic emission and subtracting point-like galactic sources, 28 cross-correlation multipole spectra were reconstructed. These data were united into the joint multipole spectrum (Fig. 5). Note the two-humped structure of the first peak. This phenomenon, discovered in the Archeops experiment, is confirmed by the WMAP data.

The detection of cross-correlation between the anisotropy and the *E*-mode of polarization, the so-called *TE* cross-correlation, is discussed in paper [20]. The significance of this cross-correlation exceeds 10σ. The authors emphasize that the discovered dependence agrees well with theoretical predictions at moderate angles ($\theta < 5^\circ$), but significantly deviates for large angles ($\theta > 10^\circ$). At large angles, an appreciable increase in the cross-correlation is detected. To explain this, cosmologists assume the presence of an ionized medium lying between us and $z \approx 20$. The optical depth for

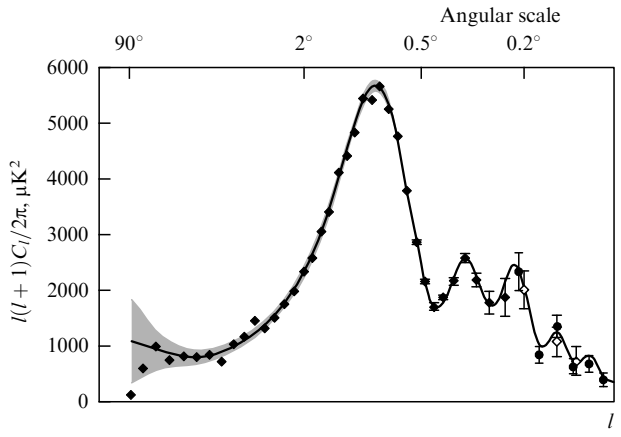

Figure 5. The anisotropy power spectrum: —— — ΛCDM (all data), ◆ — WMAP data, ◇ — CBI data, • — ACBAR data.

Thompson scattering is $\tau \approx 0.17$. As the optical depth up to quasars with $z \approx 6$ is significantly smaller than this value, this implies that the degree of ionization in the Universe apparently evolved in a complex way.

Figure 6 shows the measured cross-correlation. The strong excess at large angles (small values of the multipole number l) clearly points to the presence of an ionized plasma between us and the last scattering surface.

The two simplest models of secondary ionization are considered in paper [20]. The first model suggests the instantaneous full ionization of plasma ($x_e = 1$). In this model, the redshift of the beginning of reionization is about $z \approx 17$. But such a model would be in conflict with optical observations of quasars and measurements of the optical depth towards them. So the authors discuss another model, in which ionization evolved in a more complicated way, which leads to the beginning of reionization at $z \approx 20$. To realize such a reionization scenario, a new generation of stars is required, which should have been born at the epoch with redshift $z \approx 30$.

Finally, in paper [21] the authors discuss global cosmological parameters as inferred from the first WMAP results. Initially, a simple six-parametric E-model is considered, which can explain the observed anisotropy (the TT-spectrum) and cross-correlation between the anisotropy and the E-mode of polarization (the TE-spectrum). These parameters include the baryonic density $\Omega_b h^2$, the density of cold dark matter (CDM) $\Omega_m h^2$, the Hubble parameter h in units of 100 km s^{-1} Mpc^{-1}, the amplitude of the density fluctuation spectrum A, the optical depth for Thompson scattering during reionization τ, and, finally, the spectral index of density fluctuations n_S. The authors argue that most parameters are well determined in the framework of this model. Only two parameters provide exceptions: the spectral index n_s and the optical depth τ. There exists a clear degeneracy for these parameters. For example, the likelihood function changes by only 0.05 when varying optical depth within the range $0.11 < \tau < 0.19$. The authors also specially remark that in determining the Hubble parameter they utilized data obtained by the Hubble Space Telescope [22].

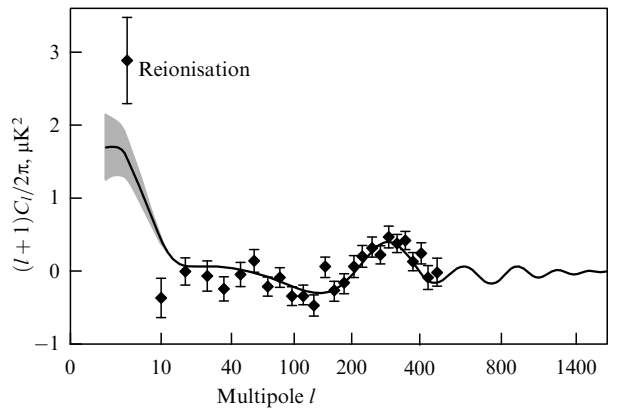

Figure 6. Cross-correlation between the anisotropy and the polarization E-mode.

The statistical analysis of the maps obtained revealed that their fluctuations are Gaussian. The authors exploited this property to study the surface of maximum likelihood by the Markov chain method. For each model, they constructed the N-dimensional distribution of the maximum likelihood function in the parameter space. The best fit value of each parameter was determined as the mean value

$$\langle p_i \rangle = \int \mathrm{d}^N p \mathbf{L}(p)\, p_i \,. \tag{6}$$

The authors claim that the simple model provides an acceptable description of the experimentally obtained TT- and TE-spectra. However, the χ^2-values for the simple model are inadmissibly large. For example, the approximation of the TT-spectrum by this model yields the value of $\chi^2 = 1.09$ normalized by the number of degrees of freedom, which means that the probability of acceptance for this model is only 3%. The best-fit to the TT- and TE-spectra yields the normalized $\chi^2 = 1.066$, which is somewhat better. Nevertheless, the probability of acceptance of this model to describe the TT- and TE-spectra is only 5%.

The χ^2-test was calculated using the formula

$$\chi^2 = -2 \ln \frac{\mathbf{L}}{v} \,,$$

where v is the number of degrees of freedom. For the model maps

$$-2 \ln \frac{\mathbf{L}}{v} = 1$$

was obtained.

The authors argue that this is due to the inability of the simple six-parametric model to fit the sharp edges the observed spectrum demonstrates at $l \approx 120$, near the first peak and at $l \approx 350$. Moreover, the authors consider the excess in the value of χ^2 to be caused by the underestimation of the noise on the maps. The excessive noise on the maps, they believe, can be due to the gravitational lens effect on the CMB anisotropy (about gravitational lens see, e.g., [23]), angular variations of the WMAP beaming, as well as the small contribution of non-gaussian noise on the maps, which appears when reconstructing two-dimensional sky maps from one-dimensional scans.

In Table 2 we now list global cosmological parameters obtained in this simple parametric model for the WMAP data.

It should be noted that cosmologists approximated experimental data assuming flat three-dimensional space, i.e., in the framework of the standard cosmological ΛCDM-model.

Table 2

Parameter	Mean value (68% c.l.)
Baryon density $\Omega_b h^2$	0.024 ± 0.001
CDM density $\Omega_m h^2$	0.14 ± 0.15
Hubble parameter h	0.72 ± 0.05
Amplitude of density perturbations A	0.9 ± 0.1
Optical depth τ	0.166 ± 0.073
Spectral index n_s	0.99 ± 0.04

In addition to these primary parameters inferred from comparison of experimental data with the theoretical model, the researchers also give a list of 16 cosmological parameters (Table 3), derived using the primary parameters, with most of them having been obtained by the CMBFAST code [17, 24] and by integrating the Friedmann equations.

These parameters should be added to the density parameter associated with Λ: $\Omega_\Lambda = 0.663$.

Besides the simplest models with six parameters, the authors [21] considered more complicated models with additional parameters, in particular, the model with the so-called running spectral index. Here, the density fluctuations were assumed to depend on the wave vector in a more complicated way than pure power law. This dependence can be approximated by a near power law with small deviation

$$n_S(k) = n_S(k_0) + \frac{dn_S}{d\ln k} \ln\frac{k}{k_0} . \quad (7)$$

The power spectrum of scalar perturbations is fixed at the wave vector value $k_0 = 0.05$ Mpc^{-1}.

The WMAP data alone are insufficient to derive the small addition to the spectral index from observations. Other results on the CMB anisotropy measurements should be included, in particular, those of the ground-based experiments ACBAR and CBI, the 2dFGRS galactic catalog, as well as data on the L_α line distribution in spectra of remote quasars.

Using only data on the CMB anisotropy would yield $dn_S/d\ln k$ equal to $-0.031\left(^{+0.023}_{-0.025}\right)$, and when including data on the L_α lines this value is $-0.031\left(^{+0.016}_{-0.017}\right)$. These results indicate that the effect (if any) is detected at the $\sim 2\sigma$ significance level. Of course, the use of data obtained in other experiments which utilized other methods somewhat decreases the obtained value of the variable spectral index.

The authors also considered the possible contribution from gravitational waves of cosmological origin to CMB anisotropy. Gravitational waves should have been generated during the inflation stage [25, 26] due to the parametric amplification of gravitational waves [27].

The gravitational wave spectrum in the model under consideration has a power-law dependence on the wave vector, and the spectral index[4] is related to the ratio of amplitudes of the two spectra as $n_T = -r/8$, where r is the ratio of two spectra at $k = 0.002$ Mpc^{-1}. The contribution of gravitational waves to the anisotropy has not been detected; only the upper limit of possible contribution from cosmological gravitational waves has been obtained. If one considers only experimental data, the upper limit is $r < 0.71$; if one imposes additional constraints (for example, by assuming the spectral index to be smaller than one), the upper limit on the power of gravitational waves in the Universe is more stringent, $r < 0.33$.

More sophisticated models of our Universe are characterized by a large amount of global cosmological parameters. Increasing the dimension of the parameter space naturally increases the accuracy of the approximation of experimental data. At the same time, many 'degeneracies' in the parameter space appear. A degeneracy can be demonstrated by the following example. The available set of experimental data in cosmology can correspond to two quite different models. For example, say, the model with a quintessence with the equation of state $w = -0.5$ and other parameters $\Omega_m = 0.47$, $h = 0.57$ fits the WMAP data just as well as the standard ΛCDM model does. Clearly, the model of quintessence with the equation of state $w = -0.5$ was rejected based on the Hubble parameter requirement to be 2σ smaller than the value inferred from the HST data [22]. On similar grounds, for example, the model with non-flat three-dimensional space and $\Omega_\Lambda = 0$, $\Omega_{total} = 1.28$, $H_0 = 32.5$ km s^{-1} Mpc^{-1} was also rejected.

Using the WMAP data combined with the 2dFGRS galactic catalog, one can significantly restrict the contribution from all three neutrinos to the total density of the Universe. At the matter dominance epoch, i.e., after $z = 3454$, neutrinos must form a large-scale structure due to gravitational instability. Simultaneously, their motion suppresses matter fluctuations at small scales. So by comparing fluctuations on scales, which are studied in the CMB anisotropy experiments, with those studied from galactic clustering, one can derive the upper limit on the total density of neutrinos. This limit is $\Omega_\nu h^2 < 0.0076$. Note that this value significantly exceeds the contribution of massless neutrinos to the total density. If neutrinos are massless, their fraction in the density parameter is $\Omega_\nu h^2 < 0.00006$.

Table 3

Parameter	Mean values (68% c.l.)
Density fluctuation amplitude in 8 Mpc σ_8	0.9 ± 0.1
Peculiar velocity measure $\sigma_8 \Omega_m^{0,6}$	0.14 ± 0.15
Baryon density Ω_b	0.047 ± 0.006
CDM density Ω_m	0.29 ± 0.07
Age of the universe T_0	13.4 ± 0.3 bln years
Redshift of reionisation z_{ri}	17 ± 5
Redshift of recombination z_r	1088 ± 1
Age of the universe at recombination T_r	372 ± 14 thous. years
Last scattering density thickness Δz_r	194 ± 2
Duration of recombination epoch Δz_r	115 ± 5 thous. years
Redshift of matter and radiation equality z_{eq}	3454 ± 388
'Sound' horizon size at recombination r_s	144 ± 4 Mpc
Angular distance to the last scattering surface d_a	13.7 ± 0.5 Gpc
Angular scale of acoustic oscillations $l_a = \pi d_a / r_s$	299 ± 2
Baryon density n_b	$(2.7 \pm 0.1) \times 10^{-7}$ cm^{-3}
Baryon to photon number density ratio η	$(6.5 \pm 0.3) \times 10^{-10}$ cm^{-3}

[4] See the last section for the discussion of spectrum of scalar perturbations and gravitational wave perturbations in the simplest inflationary model.

An interesting phenomenon was noted in paper [21]. The standard ΛCDM-model fits the experimental data well at almost all angular scales but deviates at large ($\theta \sim 60^\circ$) and small angular scales. While the discrepancy at small scales can be removed by considering the non-power-law spectrum of perturbations, the deviations at large scales seem more enigmatic. The authors discuss several explanations in the framework of modern physics but come to the conclusion that these deviations possibly signal effects of new physics.

4. Future experiments and determination of inflation parameters

Balloon, ground-based, and cosmic experiments have measured the CMB anisotropy and reliably detected its polarization. In fact, only the *E*-mode of polarization has been registered. The *B*-mode of polarization has not been detected. New experiments are in preparation, some of which are dedicated to detecting both polarization modes, some of which are designed for more detailed study of the anisotropy. When discussing experiments, so far we have touched upon only the Universe at the epoch of recombination and post-recombination. However, the primordial density perturbations and gravitational waves were generated during the inflation stage. So they must carry information on the conditions under which inflation occurred. Now let us discuss which parameters of the Universe at the inflationary stage can be inferred from studying the anisotropy and recombination of CMB.

The reader can learn about the theory of inflation in monographs [2, 3] published in Russian, or using original papers included in the collection of papers on the theory of inflation [28].

Let us consider the simplest case where inflation in the Universe is produced by one scalar field ϕ:

$$\ddot{\phi} + 3H\dot{\phi} + V'(\phi) = 0\,. \tag{8}$$

Here, the dot denotes the derivative with respect to time, and the prime denotes the partial derivative of the potential $V(\phi)$ with respect to the field variable ϕ,

$$H^2 = \frac{8\pi}{3m_{\rm Pl}^2}\left[\frac{1}{2}\,\dot{\phi}^2 + V(\phi)\right], \tag{9}$$

where $m_{\rm Pl} = 1.2 \times 10^{19}$ GeV is the Planck mass.

In most inflation models, the conditions of slow change of the field (the slow-roll approximation) hold. These conditions can be written as [29]

$$\frac{m_{\rm Pl}^2}{4\pi}\frac{H''}{H} = \eta(\phi) \ll 1\,, \tag{10}$$

$$\frac{m_{\rm Pl}^2}{4\pi}\left(\frac{H'}{H}\right)^2 = \epsilon(\phi) \ll 1\,. \tag{11}$$

If the slow-roll conditions (10) and (11) are met, one can find Fourier-amplitudes of density perturbations

$$A_{\rm d}(\phi) = \sqrt{\frac{2}{\pi}}\,\frac{1}{m_{\rm Pl}^2}\,\frac{H^2}{|H'|} \tag{12}$$

and of gravitational waves

$$A_{\rm g}(\phi) = \sqrt{\frac{1}{2\pi}}\,\frac{H}{m_{\rm Pl}} \tag{13}$$

[25, 26, 29–31]. The wavelength of a perturbation λ can be related to the scalar field ϕ as

$$\frac{{\rm d}\ln\lambda}{{\rm d}\phi} = \frac{\sqrt{4\pi}}{m_{\rm Pl}}\,\frac{A_{\rm d}(\phi)}{A_{\rm g}(\phi)}\,. \tag{14}$$

In the slow-roll approximation, density perturbation and gravitational wave spectra turn out to be close to power-law ones. The density perturbation spectrum is usually written in the form $A_{\rm d}^2 = A^2 k^{n_{\rm S}-1}$, and the gravitational wave spectrum as $A_{\rm g}^2 = B^2 k^{n_{\rm T}}$. In the case of the limiting slow-roll, the Harrison–Zel'dovich spectrum (the HZ-spectrum) is obtained, for which $n_{\rm S} = 1$ and $n_{\rm T} \ll 1$. Cosmologists also introduce the parameter

$$r = \frac{B}{A} = \sqrt{\epsilon(H_0)}\,,$$

where k is the wave vector of the corresponding perturbation and H_0 is the present-day value of the Hubble parameter.

Using the anisotropy and polarization of CMB, astronomers can reconstruct spectra of density perturbations and gravitational waves. Note that both anisotropy and polarization must be known for unambiguous reconstruction of these spectra [32].

To separate measurement of density perturbations and gravitational waves, detection of the *E*- and *B*-modes of polarization is especially useful. We recall that density perturbations contribute only to the *E*-mode, while gravitational waves generate both *E*- and *B*-modes.

Spectra of density perturbations and gravitational waves allow the reconstruction of the value of the scalar field potential driving inflation and its first derivative in a broad range of ϕ values [33]. At present, as only the anisotropy has been discovered and the *E*-mode of polarization has marginally been detected, one can find the slope of the potential driving the inflation, but unfortunately it is impossible to infer its absolute value. This may be possible in the future when new experiments on measuring the CMB anisotropy and polarization will start operating, such as PLANCK [34] and SPOrt [35].

In addition to reconstructing the inflation potential, SPOrt will be capable of solving the problem of the excessive degree of polarization at small multipole numbers, as this experiment is specially dedicated to polarization studies at low multipoles.

The PLANCK satellite will construct the all-sky map at several frequencies with a record resolution of a few angular minutes and a high sensitivity. This probably will help to solve the enigma of the double top of the first Doppler peak and in understanding the disagreement of the standard ΛCDM model with CMB anisotropy and polarization observations.

5. Conclusion

Big changes have occurred in cosmology. Twenty to thirty years ago one of the principal questions in cosmology was the determination of the topology of the Universe: is our Universe open or closed? Is the volume of our Universe infinite or finite? The answer to this problem was to measure the total density parameter Ω. The allowed range of this parameter was $0.003 < \Omega < 10$. Now, the total density of the Universe is known to within a few percent: $\Omega = 1.02 \pm 0.02$. Most other global parameters of the Universe have been measured with compatible accuracy. Observations of the

CMB anisotropy, in particular the WMAP results on the CMB anisotropy and polarization, opened up a new epoch of 'precision cosmology'. Cosmology has now become a precise science, the uncertainty in determining its main parameters approaching the accuracy of physical measurements. This allows quantitative studies of new phenomena in the Universe. One of the priorities in these studies is the investigation of quintessence, a new form of matter which as yet can not been explored in the laboratory.

New cosmic and ground-based experiments on CMB anisotropy and polarization will bring new knowledge of processes in the early Universe and will allow better understanding of physical processes at super-large scales in our Universe.

References

1. Zel'dovich Ya B, Novikov I D *Stroenie i Evolyutsiys Vselennoĭ* (Structure and Evolution of the Universe) (M.: Nauka, 1975)
2. Dolgov A D, Zel'dovich Ya B, Sazhin M V *Kosmologiya Ranneĭ Vselennoĭ* (Moscow: Izd. MGU, 1988) [Translated into English: Dolgov A D, Sazhin M V, Zeldovich Ya B *Basic of Modern Cosmology* (Gif-sur-Yvette: Editions Frontières, 1990)]
3. Linde A D *Kosmologiya i Elementarnye Chastitsy* (Cosmology and Elementary Particles) (Moscow: Nauka, 1985) [Translated into English: *Particle Physics and Inflationary Cosmology* (Chur: Harwood Acad. Publ., 1990)]
4. Weinberg S *Gravitation and Cosmology*: *Principles and Applications of the General Theory of Relativity* (New York: Wiley, 1972) [Translated into Russian (Moscow: Mir, 1975)]
5. Sazhin M V *Sovremennaya Kosmologiya v Populyarnom Izlozhenii* (Modern Cosmology in Popular Presentation) (Moscow: Editorial URSS, 2002)
6. Strukov I A et al. *Pis'ma Astron. Zh.* **18** 387 (1992) [*Sov. Astron. Lett.* **18** 153 (1992)]
7. Strukov I A et al. *Mon. Not. R. Astron. Soc.* **258** 37P (1992)
8. Smoot G F et al. *Astrophys. J.* **396** L1 (1992)
9. de Bernardis P et al. *Nature* **404** 955 (2000)
10. Benoit A et al. *Astron. Astrophys.* **399** L19 (2003); astro-ph/0210305
11. Benoit A et al. *Astron. Astrophys.* **399** L25 (2003); astro-ph/0210306
12. http://archeops03.free.fr/main_archeops/index_english.html
13. Leitch E M et al. *Nature* **420** 763 (2002); astro-ph/0209476
14. Kovac J et al. *Nature* **420** 772 (2002); astro-ph/0209478
15. Sazhin M V, Shul'ga V V *Vest. Mosk. Univ. Ser. 3 Fiz. Astron.* **37** (3) 69 (1996)
16. Sazhin M V, Shul'ga V V *Vestn. Mosk. Univ. Ser. 3 Fiz. Astron.* **37** (4) 87 (1996)
17. Seljak U, Zaldarriaga M *Phys. Rev. Lett.* **78** 2054 (1997)
18. Wilkinson Microwave Anisotropy Probe, http://map.gsfc.nasa.gov and references therein
19. Hinshaw G et al., First Year Wilkinson Microwave Anisotropy Probe (WMAP) Observations: The Angular Power Spectrum, astro-ph/0302217
20. Kogut A et al., First Year Wilkinson Microwave Anisotropy Probe (WMAP) Observations: TE Polarization, astro-ph/0302213
21. Spergel D N et al., First Year Wilkinson Microwave Anisotropy Probe (WMAP) Observations: Determination of Cosmological Parameters, astro-ph/0302209
22. Freedman W L et al. *Astrophys. J.* **553** 47 (2001)
23. Zakharov A F, Sazhin M V *Usp. Fiz. Nauk* **168** 1041 (1998) [*Phys. Usp.* **41** 945 (1998)]
24. Seljak U, Zaldarriaga M, http://physics.nyu.edu/matiasz/CMBFAST/cmbfast.html
25. Starobinsky A A *Pis'ma Zh. Eksp. Teor. Fiz.* **30** 719 (1979) [*JETP Lett.* **30** 682 (1979)]
26. Rubakov V A, Sazhin M V, Veryaskin A V *Phys. Lett. B* **115** 189 (1982)
27. Grishchuk L P *Zh. Eksp. Teor. Fiz.* **67** 825 (1974) [*Sov. Phys. JETP* **40** 446 (1974)]
28. Abbott L F, Pi S-Y *Inflationary Cosmology* (Singapore: World Scientific, 1986)
29. Copeland E J et al. *Phys. Rev. D* **48** 2529 (1993)
30. Dodelson S, Knox L, Kolb E W *Phys. Rev. Lett.* **72** 3444 (1994)
31. Starobinsky A A *Phys. Lett. B* **117** 175 (1982)
32. Sazhin M V, Benitez N *Astrophys. Lett. Commun.* **32** 105 (1995)
33. Melchiorri A et al. *Astrophys. J.* **518** 562 (1999)
34. http://astro.estec.esa.nl/SA-general/Projects/Planck/
35. SKY Polarization Observatory, http://sport.bo.iasf.cnr.it/